The electronic, structural and nonlinear optical properties of licochalcone L in the aqueous solution and gaseous phase: A DFT study

Ankit Mittal[a,1], Mudita Nagpal[b], Varun Chahal[c], Vinod Kumar Vashistha[d]

[a]Department of Chemistry, Shyam Lal College, University of Delhi, Delhi-110032, India

[b]Department of Applied Sciences, Vivekananda Institute of Professional Studies – Technical Campus, Delhi-110034, India

[c]Department of Chemistry, Deenbandhu Chhotu Ram University of Science and Technology (DCRUST), Murthal, Haryana-131309, India

[d]Department of Chemistry, Institute of Applied Sciences and Humanities, GLA University, Mathura, Uttar Pradesh-281406, India

Abstract: In the present article, various conformers of licochalcone L, a chalcone derivative extracted from the *G. inflata* root, have been analyzed in the aqueous solution and gaseous phase using calculation based on density functional theory (DFT). Nonlinear optical parameters such as dipole moment (μ), mean polarizability (α), polarizability anisotropy ($\Delta\alpha$) and the first order hyperpolarizability (β) have been estimated to examine the NLO properties of the title molecule. These parameters were found to be significantly higher than those of standard molecules, indicating the potential NLO applications of licochalcone L. The analysis of natural bond orbitals (NBO) has been carried out to characterize various intramolecular interactions. The nucleus-independent chemical shift (NICS) technique has been used to investigate the aromaticity. Further, the pK_a values have been computed for each hydroxyl group, revealing that the neutral form predominates at physiological pH, while the monoanionic form becomes predominant at pH greater than 9. The impact of solvation on the molecular electrostatic potentials and frontier molecular orbitals has been investigated for the neutral as well as monoanionic form of licochalcone L. A variety of global chemical reactivity descriptors have been calculated to highlight the structure-activity relationship.

1. Introduction

Medicinal compounds derived from natural products always favored to synthetic ones due to their little or no side effects on healthy tissues. The chalcones, also known as "open chain flavonoids," are regarded as one of the significant subgroups of the flavonoid family. The basic skeleton of chalcone consist of two aromatic rings, named A and B, connected with a propenal bridge, as shown in Figure 1. A number of chalcone derivatives were synthesized as well as extracted from the plant species, for example, echinatin, licochalcone A, B, C, D, E, F, H, I etc. These have reportedly been shown to have a variety of pharmacological effects, including antioxidant, anti-cancer, anti-diabetic, anti-inflammatory, anti-obesity, anti-bacterial, anti-

parasitic, anti-angiogenic, anti-arthritic, anti-osteogenic, and neuroprotective, to mention a few [1-8].
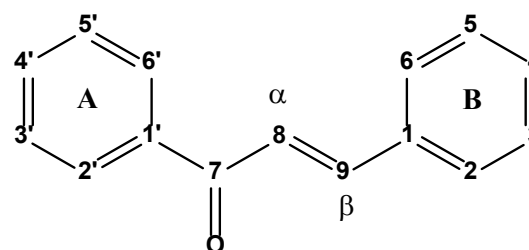
Figure 1 Basic skeleton of chalcone with atomic labeling

In the recent past, Ali and co-workers identified a new chalcone derivative, licochalcone L, from the

---

[1] Corresponding Author

e-mail: ankit.mittal@shyamlal.du.ac.in

G. inflata root's chloroform extract by using a variety of chromatography methods including flash chromatography, column chromatography and high-performance liquid chromatography (HPLC). Further, they elucidated its chemical structure, as depicted in Figure 2, using several techniques like ^{1}H-NMR, ^{13}C-NMR (1D and 2D), [1]H-^{1}H correlated spectroscopy (COSY), heteronuclear multiple bond correlation (HMBC) and high-resolution electrospray ionization mass spectrometry (HRESIMS) [9].
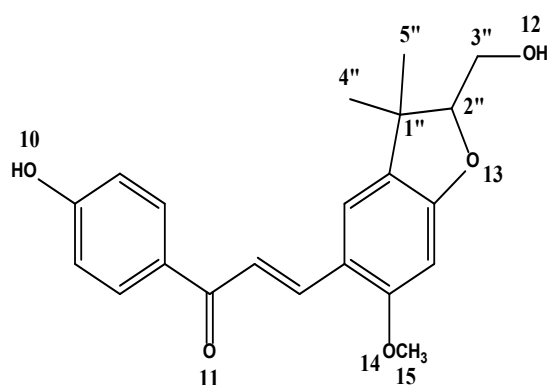
Figure 2 Structure of Licochalcone L

Previously, we have studied the structural, electronic and nonlinear optical (NLO) properties of a few retrochalcones like licochalcone A, B, C, D and E, and echinatin, using DFT calculations [10-11]. In this work, firstly, we found out the most stable conformer of licochalcone L in the aqueous solution and gaseous phase. Then, we studied the electronic and nonlinear optical properties of this conformer.

In this study, the calculated pK_a values for each hydroxyl group found in licochalcone L are presented. When examining the antioxidant processes of polyphenolic substances, the pK_a values are crucial. Several reactive nitrogen, oxygen and sulphur species are effectively neutralized by the powerful free radical scavenging properties of polyphenols [4,12]. These mechanisms include sequential proton loss electron transfer (SPLET), sequential proton loss hydrogen atom transfer (SPLHAT), and sequential double proton loss electron transfer (SdPLET), in which first step is the deprotonation of hydroxyl group. To further emphasize the structure-activity relationship, we have estimated a variety of global chemical reactivity descriptors (GCRD), looked

into frontier molecular orbitals, and examined molecular electrostatic potentials.

In this study, we delve into the multifaceted aspects of licochalcone L, employing advanced computational methods based on DFT. Our investigation spans both the aqueous solution and gaseous phase, allowing us to gain insights into the molecule's behavior in different environments. The significance of this research extends beyond theoretical exploration; it holds promise for practical applications in fields ranging from materials science to optoelectronics.

2. Computational Method

Three parameter density functional, B3LYP, was employed for the DFT computations [13-15]. The geometry of each structure was completely optimized using the Gaussian 09W suite [16] at the B3LYP/6-311++G** level. After that, the stationary points were confirmed, and harmonic frequency calculations were used to optimize the zero-point energy corrections [17].

The impact of bulk solvent was examined using the universal implicit SMD model [18]. Compared to previous models, this one offer better solvation Gibbs energies [19]. Using the NBO module, the analysis of natural bond orbitals was conducted to determine the Wiberg bond order and the type of intramolecular interactions present in the given molecule [20-26]. At GIAO-SCF/6-311++G(d,p) level of theory, the NICS values were determined [27].

3. Results and discussion
3.1. Relative Gibbs energies of licochalcone L conformers

The retrochalcones may exist in *E* and *Z* conformations with in-plane and out-of-plane conformers. From our earlier work, it has been observed that the in-plane *E* form conformers constitute major population of the aqueous solution and gaseous phase [10-11]. Further, among the *E* form conformers, s-cis conformers are relatively more populated and possess less energy than those of the s-trans conformers. Therefore, we have considered s-cis conformers of the *E* form of licochalcone L. By reorienting the two hydroxyl groups in the title molecule, a total of six conformers were produced. All were optimized in

Ankit Mittal, Mudita Nagpal, Varun Chahal, Vinod Kumar Vashistha

the aqueous solution and gaseous phase at B3LYP/6-311++G** level. Figure 3 illustrates the optimized geometries in the gaseous phase. The relative Gibbs energies and populations of all six conformers of licochalcone L in the aqueous

solution and gaseous phase are tabulated in Table 1. Table S1 of the Supporting Information contains the computed Gibbs energy for each of these conformers in both the aqueous solution and gaseous phase.
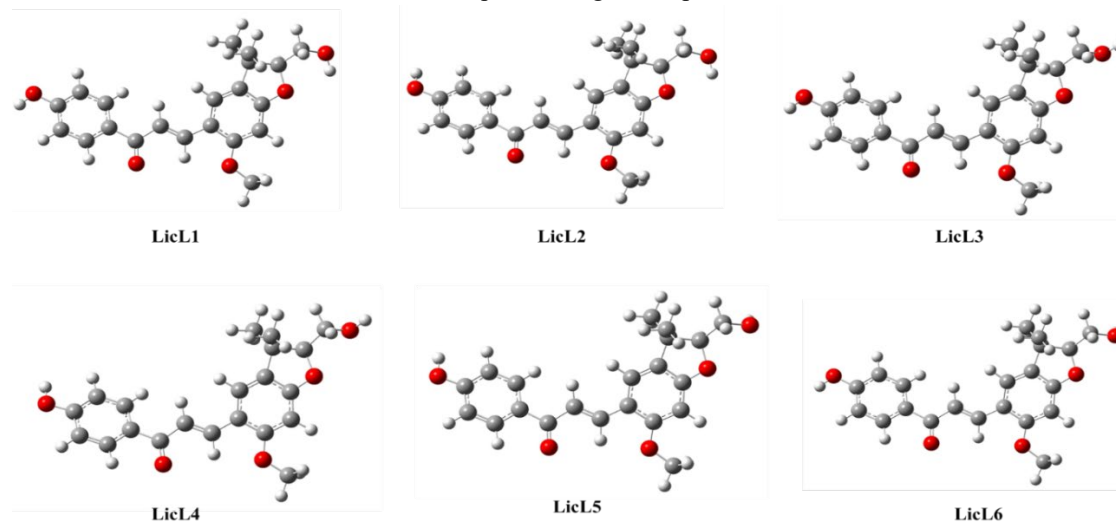
Figure 3 The gas-phase optimized geometries of licochalcone L conformers

Table 1. Relative Gibbs energies and percentage of all the conformers (LicL1 - LicL6) of licochalcone L in the aqueous solution and gaseous phase

Conformer	Relative Gibbs energy (kcal mol^{-1})		Percentage (%)	
	Gaseous phase	**Aqueous solution**	**Gaseous phase**	**Aqueous solution**
LicL1	0.0	-21.8	56.8	18.8
LicL2	0.2	-22.0	38.7	21.2
LicL3	1.8	-22.5	1.8	12.1
LicL4	2.0	-22.2	1.2	13.7
LicL5	2.6	-22.3	0.6	18.4
LicL6	2.3	-22.1	0.9	16.0

It can be observed that LicL1 conformer is the most stable and most populated in the gaseous phase. In aqueous solution, the difference between Gibbs free energy as well as population of LicL1 and LicL2 conformers is very less. On comparing both the parameters in the aqueous solution and gaseous phase for LicL1 and LicL2 conformers, we found that LicL1 is the conformer which is to be taken to study electronic properties of licochalcone L.

The Gibbs energy of the **LicL1** conformer in the gaseous phase, i.e., -1189.570872 Ha (1M standard state) is the reference for the Gibbs energies in both the aqueous solution and gaseous phase.

3.2. Optimized geometries
3.2.1. Neutral molecule

The optimized geometry of neutral form of licochalcone L in the gaseous phase is depicted in Figure 4. Table S2 lists a few chosen geometrical

characteristics of the under-investigation molecule, including bond angles, bond lengths, dihedral angles, and Wiberg bond orders.
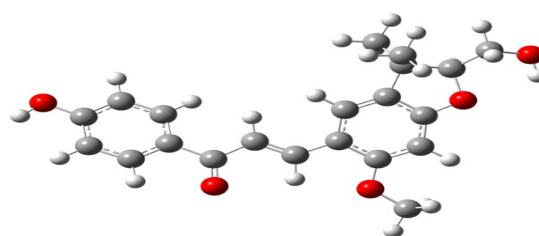
Figure 4 The optimized gas phase geometry of licochalcone L

The Wiberg bond order values of C7-O11 and C8-C9 indicate the extent of delocalization in the molecule via propenal bridge between ring A and B. These values further decrease on solvation. The Wiberg bond order of the two hydroxyl groups present in the molecule also decreases in water due

to interactions with the solvent molecules. Moreover, the effect of substituent attached to the ring B on the planarity of the molecule could be seen from the dihedral angles listed in Table S2. The dihedral angle for O11-C7-C8-C9 was found to be 5.4 degrees in the gas phase, which get reduced to 3.3 degrees in the aqueous solution. A significant change of 10 degrees was observed in the dihedral angle of C2"-C3"-O12-H12.

The calculated partial charges *viz*. natural, Mulliken, and ESP, on each atom of licochalcone L are given in Table S4. From the analysis of natural charges, we found that the carbon atoms adjacent to oxygen atom, i.e., C4', C2, C7, C4 and C2", are positively charged and others are negatively charged. Further, the most negatively charged atom of the molecule includes O10 and O12, and the hydrogen linked to these oxygen atoms are observed to be most positively charged atoms.

3.2.2. Anion
The gas-phase optimized geometry of the monoanionic form of licochalcone L is depicted in Figure 5. Table S3 lists a few chosen geometrical characteristics, including bond angles, bond lengths, dihedral angles, and Wiberg bond orders.
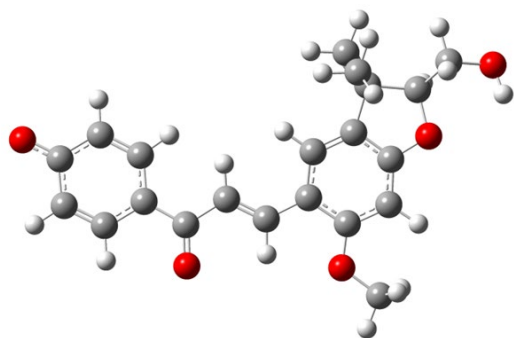
Figure 5 The optimized geometry of monoanionic form of licochalcone L in the gaseous phase

Table S3 displays various changes in the bond parameters caused by the deprotonation of the hydroxyl group linked to ring A of the molecule. In comparison to the neutral form of the molecule, the Wiberg bond order of C7-O11 is reduced. This is because following deprotonation, O10 underwent a delocalization of the negative charge. This value further decreases on solvation. Moreover, the dihedral angle for O11-C7-C8-C9 was found to be

0.7 degrees in the gaseous phase and 2.7 degrees in the aqueous solution.

The estimated partial charges *viz*. natural, Mulliken, and ESP, on each atom of the monoanionic form of licochalcone L are given in Table S5. In comparison to the neutral form, the negative charge on the two most negatively charged atoms, O10 and O12, is higher in the monoanionic form. In addition, the natural charge value on C4' is increased in the monoanionic form, as it is directly attached to the deprotonated site.

3.3. Natural bond orbital analysis
The study of various interactions between the antibonding and bonding orbitals of a molecule has been greatly aided by the development of NBO analysis as a computational tool. NBO analysis was carried out in both the aqueous solution and gaseous phase. Tables S6 and S7 list the significant interactions as well as their interaction energies.

The overlapping of π(C-C) and π^*(C-C) orbitals in the phenyl rings is the primary cause of the charge delocalization, which results in intramolecular charge transfer. Further, π(C8-C9) to π^*(C1-C2) electron density transfer and vice-versa indicates the conjugation between olefinic bond and ring B of licochalcone L. Additionally, oxygen atoms' lone pairs contribute electron density majorly to the σ^* orbitals. The lone pairs of carbonyl oxygen transfer electron density primarily to σ^*(C1'-C7) and σ^*(C7-C8) orbitals with almost same interaction energies. Only slight changes are observed in the interaction energies in aqueous solution. All these substantial interactions between donor and acceptor orbitals of the title molecule excited us to study the nonlinear optical properties.

3.4. Nonlinear optical properties
Chalcone derivatives have gained much attention of many research groups due to their excellent NLO parameters. The NLO materials are found wide range of applications in frequency doubling and mixing, lasers, optical sensors, efficient data storage and many others [28-29]. The enhanced NLO properties of chalcone derivatives is attributed to various electron donors and electron acceptors attached to the aromatic rings of the chalcone framework, which enhanced the π-conjugation in the compound through the bridge connecting two aromatic rings.

In order to access the NLO characteristics of the molecule, various NLO parameters *viz.* the dipole moment (μ), polarizability anisotropy ($\Delta\alpha$), mean polarizability (α), and the first order hyperpolarizability (β), are computed with the help of following relations [30-32]:

$$\mu = \left(\mu_x^2 + \mu_y^2 + \mu_z^2\right)^{\frac{1}{2}}$$

$$\alpha = \frac{1}{3}\left(\alpha_{xx} + \alpha_{yy} + \alpha_{zz}\right)$$

$$\Delta\alpha = \frac{1}{\sqrt{2}}\left[\left(\alpha_{xx} - \alpha_{yy}\right)^2 + \left(\alpha_{yy} - \alpha_{zz}\right)^2 \right.$$
$$+ \left(\alpha_{zz} - \alpha_{xx}\right)^2$$
$$\left. + 6\left(\alpha^2_{xy} + \alpha^2_{xz} + \alpha^2_{yz}\right)\right]^{\frac{1}{2}}$$

$$\beta = \left(\beta_x{}^2 + \beta_y{}^2 + \beta_z{}^2\right)^{\frac{1}{2}}$$

where, β_x, β_y and β_z are calculated as

$$\beta_x = \beta_{xxx} + \beta_{xyy} + \beta_{xzz}$$

$$\beta_y = \beta_{yyy} + \beta_{yzz} + \beta_{xxy}$$

$$\beta_z = \beta_{zzz} + \beta_{xxz} + \beta_{yyz}$$

All these NLO parameters were also computed for two reference compounds, i.e., *para*-nitroaniline and urea, as tabulated in Table 2. The values of *x, y* and *z* components of all the NLO parameters in the aqueous solution and gaseous phase are listed in Table S8.

It can be seen that the average polarizability of licochalcone L in the gaseous phase is roughly nine times more than that of urea and three times greater than that of *para*-nitroaniline. In aqueous solution, this value is increased by 1.5 times for licochalcone L. Next, in the gaseous phase, the polarizability anisotropy of licochalcone L is about 18 times more than that of urea and three times greater than that of *para*-nitroaniline. This value of licochalcone L is 1.4 times higher in aqueous solution than it is in the gas phase. Moreover, the first hyperpolarizability of the title molecule in the gas phase is 42 times to that

of the urea and 2.3 times to that of the *para*-nitroaniline. In aqueous solution, this value of first hyperpolarizability for licochalcone L is increased by 4.3 times to that of the gas phase value. All these findings suggest that licochalcone L has excellent NLO features and might be recommended for more NLO applications.

3.5. NICS: a criterion for aromaticity

The aromaticity and antiaromaticity of licochalcone L were determined utilizing the nucleus-independent chemical shift (NICS) approach [33]. The NICS values of the rings A and B of licochalcone L and benzene were calculated above, at, and below their respective centers. NICS(0) is used to represent the NICS value at the ring's center. Further, the NICS values were calculated up to 2 Å with a gap of 0.5 Å above and below the ring's center, as tabulated in Table 3. The NICS values above and below the plane are represented with positive and negative signs, respectively.

The aromatic nature of both rings of licochalcone L is indicated by the fact that all of the NICS values are negative. It has been suggested that NICS(1) or NICS(-1), should be considered for the comparative study with other compounds. This is as a result of lower impact of σ framework at 1 Å. The NICS(1) value of both the rings of licochalcone L is found to be less than that of the benzene, which indicate that the licochalcone L is less aromatic than benzene. Further, the NICS(1) value of ring A is -9.4 ppm and that of ring B is -7.8 ppm. Thus, ring A is more aromatic than ring B owing to the presence of substituent at ring B. In addition, the effect of substituent is also observed when we compare the NICS(-1) and NICS(1) values of ring B. The NICS(-1) is slightly higher than that of NICS(1) value.

3.6. Gas-phase basicity and pK_a

Licochalcone L contain two OH groups, one of which is directly attached to 4' position of ring A and other is present at 3" position of the substituent attached to ring B, as shown in its structure. These two OH groups may get deprotonated according to the pH of the medium. In accordance with the methods used in our prior work, we have thus determined the pK_a value corresponding to each hydroxyl group present in licochalcone L [10-11]. The thermodynamic cycle utilized for the

Ankit Mittal, Mudita Nagpal, Varun Chahal, Vinod Kumar Vashistha

calculations is represented in Scheme 1. The GPB is abbreviated for "gas-phase basicity" and it is defined as the negative of Gibbs energy change for

protonating monoanionic form of licochalcone L in the gaseous phase.

Table 2 The computed* dipole moment (μ, in Debye), average polarizability (α, in esu), polarizability anisotropy ($\Delta\alpha$, in esu), the first hyperpolarizability (β, in esu) of licochalcone L, urea and *para*-nitroaniline in the gaseous phase and aqueous solution (in parentheses)

Compound	NLO Parameters			
	μ	α ($\times 10^{-24}$)	$\Delta\alpha$ ($\times 10^{-24}$)	β ($\times 10^{-30}$)
LicL1	1.70 (3.84)	45.82 (68.52)	38.78 (55.69)	32.71 (139.04)
Urea	3.88 (6.38)	5.05 (6.51)	2.11 (2.89)	0.78 (0.66)
para-nitroaniline	7.48 (13.13)	15.10 (26.46)	13.31 (31.69)	14.27 (86.44)

*μ: 1 au = 2.54 Debye; α and $\Delta\alpha$: 1 au = 0.1482 $\times 10^{-24}$ esu; β: 1 au = 8.6393 $\times 10^{-33}$ esu

Table 3 Computed NICS values (in ppm) above, at and below the center of both the rings A and B of licochalcone L and benzene

NICS*	A-ring	B-ring	Benzene
NICS(-2)	-4.3	-3.7	-4.9
NICS(-1.5)	-6.8	-5.7	-7.7
NICS(-1)	-9.4	-8.0	-10.3
NICS(-0.5)	-9.8	-8.5	-10.2
NICS(0)	-8.5	-7.7	-8.3
NICS(0.5)	-9.5	-8.2	-10.2
NICS(1)	-9.4	-7.8	-10.3
NICS(1.5)	-7.0	-5.8	-7.7
NICS(2)	-4.4	-3.8	-4.9

*Figures in parentheses are the distance (Å) from the center of the ring.
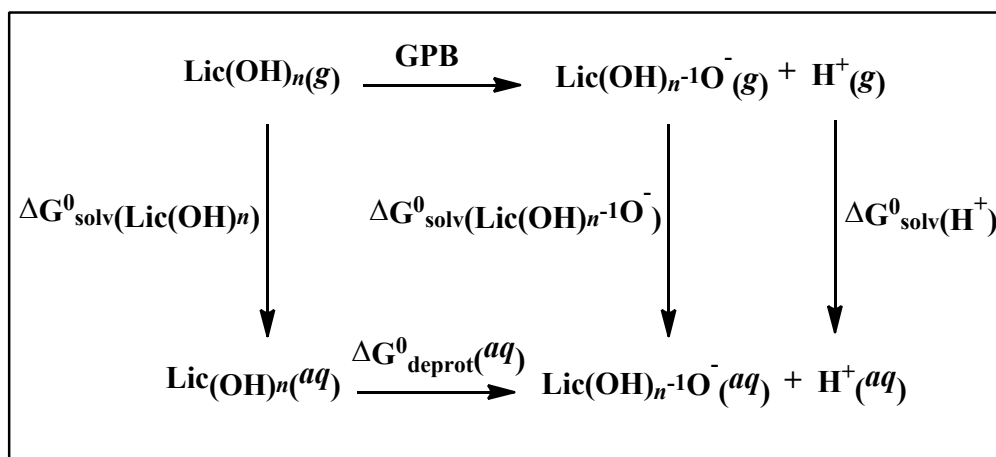
Scheme 1 Thermodynamic cycle for determining the GPB and first pK_a values of the deprotonation sites in licochalcone L (Lic(OH)$_n$)

The basicity of licochalcone L and its pK_a values in the aqueous solution were estimated using Scheme 1 as follows

$$\Delta G^0{}_{deprot}(aq) = GPB$$
$$+ \Delta G^0{}_{solv}(Lic(OH)_{n-1}O^-)$$
$$+ \Delta G^0{}_{solv}(H^+)$$
$$- \Delta G^0{}_{solv}(Lic(OH)_n)$$

Ankit Mittal, Mudita Nagpal, Varun Chahal, Vinod Kumar Vashistha

$$pK_a = \frac{\Delta G^0{}_{deprot}(aq)}{RTln10}$$

where $\Delta G^0{}_{solv}(H^+)$, the proton's standard hydration Gibbs energy at 298.15 K and 1 atm was considered to be -265.9 kcal mol^{-1} [34-35]. $\Delta G^0{}_{solv}(Lic(OH)_n)$ and $\Delta G^0{}_{solv}(Lic(OH)_{n-1}O^-)$ represent the solvation energy of neutral and monoanionic form of licochalcone L, respectively. Table S9 in the supporting information lists the Gibbs energies of the monoanionic and dianionic forms of licochalcone L.

Firstly, we calculated the GPB and the pK_a value corresponding to each OH group present in licochalcone L by employing Scheme 1. The pK_a value of hydroxyl group at 4' position was found to be 8.9 and that of 3" position was 22.2, as listed in Table 4. Therefore, the first deprotonation will take place from the hydroxyl group present at 4' position and results into the formation of monoanion represented as Ia in Table 4. The lower pK_a value of hydroxyl group at 4' position is due to the resonance stabilized resulting monoanionic form.

Next, the second pK_a for deprotonating the OH group at 3" position from the monoanionic form (Ia) was evaluated using the equation,

$$\Delta G^0{}_{deprot}(aq)$$
$$= GPB + \Delta G^0{}_{solv}(Lic(OH)_{n-2}O_2^{2-})$$
$$+ \Delta G^0{}_{solv}(H^+)$$
$$- \Delta G^0{}_{solv}(Lic(OH)_{n-1}O^-)$$

The loss of proton from the hydroxyl group present at 3" position of the monoanionic form (Ia) leads to the formation of dianion (Ic) and the corresponding pK_a value was computed to be 22.4, as shown in Table 4. As a result, it may be said that licochalcone L exists in the neutral form at physiological pH and that the monoanionic form predominates at pH values higher than 9. The pK_a values help in determining the antioxidant activity of polyphenols in different pH range.

Table 4 Estimated gaseous and aqueous phase basicities (kcal mol^{-1}) and pK_a values of licochalcone L

Reaction			GPB	$\Delta G^0{}_{deprot}(aq)$	pK_a
LicL	→ Ia + H$^+$		323.7	12.1	8.9 (pK_{a1})
LicL	→ Ib + H$^+$		354.9	30.2	22.2 (pK_{a1})
Ia	→ Ic + H$^+$		390.8	30.5	22.4 (pK_{a2})

Ankit Mittal, Mudita Nagpal, Varun Chahal, Vinod Kumar Vashistha
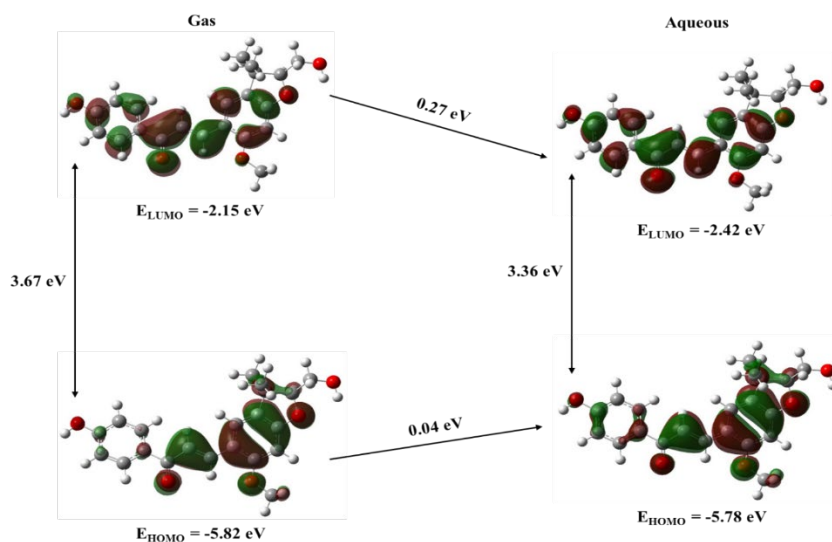
Figure 6 HOMO-LUMO diagrams of licochalcone L in the gaseous phase (left) and in the aqueous solution (right) with their respective energies and energy gaps (in eV).
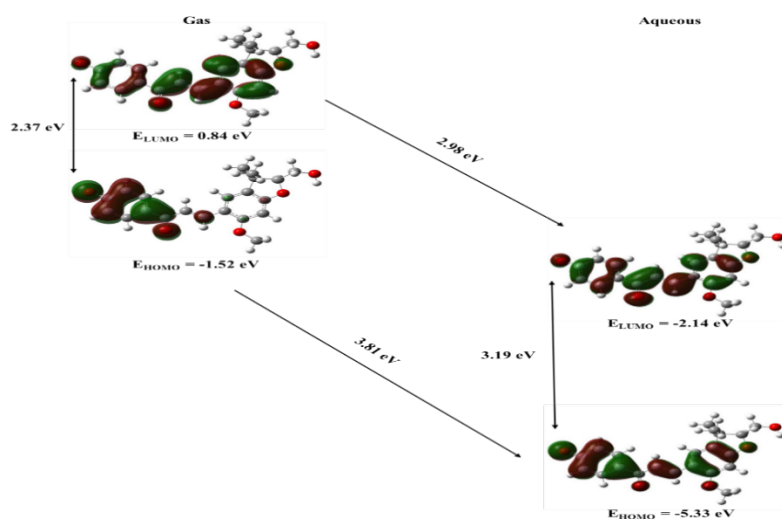
Figure 7 HOMO-LUMO diagrams of monoanionic form of licochalcone L in the gaseous phase (left) and aqueous solution (right) with their corresponding energies and energy gaps (in eV).

3.7. Frontier molecular orbitals analysis

The electrical characteristics and reactivity of licochalcone L and its monoanionic form were studied using frontier molecular orbital studies. The highest occupied molecular orbital (HOMO) and lowest unoccupied molecular orbital (LUMO) of licochalcone L along with their respective energies and energy gaps computed at the B3LYP/6-311++G** level are presented in Figure 6.

It can be observed that HOMO of the title molecule is concentrated on the B ring and the propenal bridge, with a small delocalization on the substituent, indicating a π orbital. With the exception of the connected substituent, the LUMO is delocalized throughout the entire molecule, denoting a π^* orbital. The HOMO-LUMO gap has a value of 3.67 eV and falls to 3.36 eV upon solvation. This is mainly because the LUMO energy was reduced to -2.42 eV. This demonstrates that the molecule in the aqueous solution

demonstrates greater electron accepting characteristics and increased chemical reactivity.

In the monoanionic form of the molecule, as shown in Figure 7, the HOMO is concentrated over ring A and the keto-ethylenic bridge, while LUMO is delocalized throughout the entire molecule, except the attached substituent. Thus, the HOMO and LUMO can be characterized as π and π^* orbitals, respectively. It can be observed that for the anionic form, both HOMO and LUMO have very high energies but in aqueous solution, the energies of these orbitals decreases to a greater extent due to the interaction of the monoanionic form with the water molecules. The HOMO-LUMO gap for the anion is smaller as compared to that of the neutral molecule, which indicates that anion is more polarizable.

3.8. Global chemical reactivity descriptors (GCRD)

Next, a comparison of the chemical reactivity of licochalcone L was made in the aqueous solution and gaseous phase by computing various global chemical reactivity descriptors (GCRD) including global chemical hardness (η), global chemical potential (μ), global electrophilicity (ω), electronegativity (χ), and global nucleophilicity (N) indices, as listed in Table 5. These descriptors were all calculated using the formulas below [10, 36-40]:

$$\eta = \frac{IP - EA}{2}$$

$$\mu = \frac{IP + EA}{2}$$

$$\chi = -\mu$$

$$\omega = \frac{\mu^2}{2\eta}$$

$$S = \frac{1}{2\eta}$$

$$N = -(IP_{licochalcone} - IP_{tetracyanoethylene})$$

Following are the relationships between the HOMO and LUMO energies, and the vertical ionization potential (IP) and electron affinity (EA) respectively [41]:

$$IP = -E_{HOMO}$$

$$EA = -E_{LUMO}$$

Further, the global nucleophilicity index (N) of licochalcone L was determined as the negative of the IP value relative to that of the tetracyanoethylene. The same level of theory was used to compute all the parameters for benzene in the gaseous phase for a comparison analysis, as shown in Table 5. Table S10 of the Supporting Information lists the energy characteristics of benzene and licochalcone L.

All these descriptors are regarded as very significant for the bioactivity of a molecule. The global chemical hardness of licochalcone L in the gas phase as well as aqueous solution was observed to be less than that of the benzene indicating high chemical reactivity of licochalcone L. Moreover, the global electrophilicity of licochalcone L is found be almost twice of the benzene molecule in the gaseous phase which further increases in the aqueous solution. This suggests better electrophilic nature of licochalcone L. Furthermore, the global nucleophilicity is observed to be higher than that of the benzene indicating good nucleophilic nature of the title molecule in comparison to that of the benzene.

3.9. Molecular electrostatic potential (MEP)

The MEPs of the title compound and its monoanionic form were calculated in both phases to evaluate the regions of neutral, positive and negative potentials. The blue region signifies the site of nucleophilic attack, whereas red colored region signifies the site of electrophilic attack [42]. The MEP maps of neutral and monoanionic form of licochalcone L in the aqueous solution are displayed in Figure 8.

It can be observed that the blue region is clearly seen near hydrogen atom of the hydroxyl groups as well as other alkyl groups, whereas red region is largely localized near the oxygen atoms in the molecule. In the neutral form, the red colored region near carbonyl group indicate that the electrophile would prefer to attack at this position. In the monoanionic form, the red color is observed

over ring A of the title compound, which suggest that the electrophile would prefer to attack at ring A.

Further, the computed MEP on each atom of the neutral and monoanionic form of title compound are tabulated in Table S11. Among both the nucleus

of dissociating protons, i.e., O10 and O12, the MEP is observed to be lower on the O10 than O12. Furthermore, this is also observed to follow the same order as that of the pK_{a1} value of each deprotonation site, as calculated in Table 4.

Table 5 Comparison of global chemical reactivity descriptors (eV) of licochalcone L with those of benzene

Compound	Medium	η	μ	χ	ω	S^*	N
LicL1	Gas	1.84	-3.98	3.98	4.32	0.27	3.68
	Aqueous	1.68	-4.10	4.10	5.01	0.30	3.72
Benzene	Gas	3.30	-3.78	3.78	2.16	0.16	2.42

*Softness (S) is given in e^{-1}V^{-1}
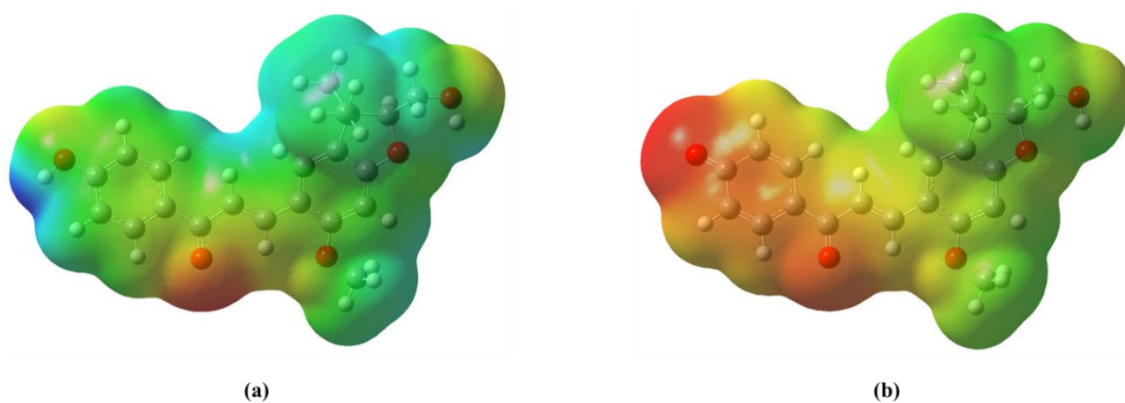
Figure 8 MEP maps of (a) the neutral [-8.590×10^{-2} (red) to 8.590×10^{-2} (blue)] and (b) monoanionic form [-0.201 (red) to 0.201 (blue)] of licochalcone L mapped on the total electron density surface at an isovalue of 0.0004 au in the aqueous solution.

3.10. Electrostatic potential (ESP) charges

Next, we have analyzed the ESP charge on each atom to identify the atom position preferable for electrophilic and nucleophilic attack in licochalcone L. Table S4 lists the ESP charge on each atom of the title molecule. Among the carbon atoms of both the rings A and B, the atoms with most negative ESP charge includes C3' and C5' of ring A having ESP charges -0.421 and -0.283, respectively; and C3 and C5 of ring B having ESP charges -0.502 and -0.396, respectively, in the gaseous phase. In aqueous solution, the ESP charges on these atoms becomes more negative. Ring B is less reactive to an electrophilic attack due to steric hindrance. As a result, in both the aqueous solution and gaseous phase, it is found that the C3' and C5' sites are the most likely sites for an electrophilic attack.

Moreover, the site having highest positive ESP charge of 0.625 in the gas phase and 0.734 in the

aqueous solution, is C7, which makes it most probable for nucleophilic attack. The absence of leaving group at this location restrict the nucleophilic substitution reaction at this position but nucleophilic addition could take place at C7 by hard nucleophiles.

4. Conclusions

The electronic, structural and NLO characteristics of a chalcone derivative named licochalcone L, extracted from the *G. inflata* root, were the main emphasis of this study. Among various conformers of licochalcone L, the most stable and relatively more populated conformer were selected by employing density functional theory (DFT) calculations at B3LYP/6-311++G** level in the aqueous solution and gaseous phase, and further properties were investigated with that conformer.

The pK_a value was calculated corresponding to each hydroxyl group present in licochalcone L. It was

found that the neutral form of licochalcone L exist as the physiological pH and the monoanionic form predominates at pH greater than 9. The propenal bridge, which connects the two ring systems, was shown to have substantial intramolecular charge transfer interactions in the NBO study. NICS parameters were used to discuss the diamagnetic ring current in the aromatic ring systems.

The nonlinear optical (NLO) parameters were found to be much higher than that of the standard molecules, i.e., urea and *para*-nitroaniline. Further, these parameters value increased many-folds on moving from gaseous phase to aqueous solution. These suggest the significance of title molecule for the NLO applications. Frontier molecular orbitals analysis were performed for the neutral as well as monoanionic form of licochalcone L. The HOMO and LUMO were characterized as π and π^* orbitals, respectively. Additionally, molecular electrostatic potential maps were employed to assess the different nucleophilic and electrophilic locations for the non-covalent interactions. In addition, the site of attack for the nucleophile and electrophile was examined with the help of electrostatic potential charge on each atom.

The advantages of the present study lie in its comprehensive investigation of the electronic, structural, and NLO properties of licochalcone L. The scientific contribution includes providing insights into the molecule's behavior in different environments, its potential as an NLO material, ionization behavior, intramolecular interactions, aromaticity, and reactivity descriptors. These findings could have implications for various fields, including materials science, medicinal chemistry, and molecular design.

Competing interests
The authors declare no conflict of interest.

References
[1] A. Mittal, R. Kakkar, The effect of solvent polarity on the antioxidant potential of echinatin, a retrochalcone, towards various ROS: a DFT thermodynamic study, Free Radical Research 54 (2020) 777-786.

[2] A. Mittal, R. Kakkar, Synthetic methods and biological applications of retrochalcones isolated from the root of Glycyrrhiza species: A review, Results in Chemistry 3 (2021) 100216.

[3] A. Mittal, R. Kakkar, The antioxidant potential of retrochalcones isolated from liquorice root: A comparative DFT study, Phytochemistry 192 (2021) 112964.

[4] A. Mittal, V.K. Vashistha, D.K. Das, Recent advances in the antioxidant activity and mechanisms of chalcone derivatives: A computational review, Free Radical Research 56 (2022) 378-397.

[5] Y. Murti, A. Goswam, P. Mishra, Synthesis and antioxidant activity of some chalcones and flavonoids, International Journal of PharmTech Research 5 (2013) 811–818.

[6] Y. Murti, D. Pathak, K. Pathak, Green chemistry approaches to the synthesis of flavonoids, Current Organic Chemistry 25 (2021) 2005–2027.

[7] J. Gupta, R. Gupta, B. Varshney, Green Approaches of Flavonoids in Cancer: Chemistry, Applications, Management, Healthcare and Future Perspectives, Journal of Pharmaceutical Research International 33 (2021) 130–143.

[8] A. Shrivastava, J.K. Gupta, M.K. Goyal, Flavonoids and antiepileptic drugs: a comprehensive review on their neuroprotective potentials, Journal of Medical Pharmaceutical and allied Sciences 11 (2022) 4179-4186.

[9] Z. Ali, M. Hawwal, M.M.A. Ahmed, B. Avula, A.G. Chittiboyina, J. Li, C. Wu, C. Taylor, Y.M. Chan, I.A. Khan, Licochalcone L, an undescribed retrochalcone from Glycyrrhiza inflata roots, Natural Product Research 36 (2021) 200-206.

[10] A. Mittal, R. Kakkar, A theoretical assessment of the structural and electronic features of some retrochalcones, International Journal

of Quantum Chemistry 121 (2021) e26797.

[11] A. Mittal, S.P. Devi, R. Kakkar, A DFT study of the conformational and electronic properties of echinatin, a retrochalcone, and its anion in the gas phase and aqueous solution, Structural Chemistry 31 (2020) 2513-2524.

[12] A. Mittal, V.K. Vashistha, D.K. Das, Free radical scavenging activity of gallic acid toward various reactive oxygen, nitrogen, and sulfur species: A DFT approach, Free Radical Research 57 (2023) 81-90.

[13] A.D. Becke, Density-functional exchange-energy approximation with correct asymptotic behaviour, Physical Review A 38 (1988) 3098-3100.

[14] C. Lee, W. Yang, R.G. Parr, Development of the Colle-Salvetti correlation-energy formula into a functional of the electron density, Physical Review B: Condensed Matter and Materials Physics 37 (1988) 785-789.

[15] S.H. Vosko, L. Wilk, M. Nusair, Accurate spin-dependent electron liquid correlation energies for local spin density calculations: a critical analysis, Canadian Journal of Physics 58 (1980) 1200-1211.

[16] M.J. Frisch, G.W. Trucks, H.B. Schlegel, Gaussian, Inc., Wallingford CT, Gaussian 09, Revision C.01, 2009.

[17] S.P. Devi, A. Mittal, R. Kakkar, Computational Studies on Reactions of Some Organic Azides with C− H Bonds, ChemistrySelect 6 (2021) 4368-4381.

[18] A.V. Marenich, C.J. Cramer, D.G. Truhlar, Universal solvation model based on solute electron density and on a continuum model of the solvent defined by the bulk dielectric constant and atomic surface tensions, The Journal of Physical Chemistry B 113 (2009) 6378-6396.

[19] G. Saielli, Differential solvation free energies of oxonium and ammonium ions: insights from quantum chemical calculations, The Journal of Physical Chemistry A 114 (2010) 7261-7265.

[20] J.E. Carpenter, F. Weinhold, Analysis of the geometry of the hydroxymethyl radical by the "different hybrids for different spins" natural bond orbital procedure, Journal of Molecular Structure: THEOCHEM 169 (1988) 41-62.

[21] E.D. Glendening, A.E, Reed, J.E. Carpenter, F. Weinhold, NBO Version 3.1, 2009.

[22] A.E. Reed, F. Weinhold, Natural bond orbital analysis of near-Hartree-Fock water dimer, The Journal of Chemical Physics 78 (1983) 4066-4073.

[23] A.E. Reed, R.B. Weinstock, F. Weinhold, Natural population analysis, The Journal of Chemical Physics 83 (1985) 735-746.

[24] A.E. Reed, L.A. Curtiss, F. Weinhold, Intermolecular interactions from a natural bond orbital, donor-acceptor viewpoint, Chemical Reviews 88 (1988) 899-926.

[25] F. Weinhold, C.R. Landis, Natural bond orbitals and extensions of localized bonding concepts, Chemistry Education Research and Practice 2 (2001) 91-104.

[26] K.B. Wiberg, Application of the Pople-Santry-Segal CNDO method to the cyclopropylcarbinyl and cyclobutyl cation and to bicyclobutane, Tetrahedron 24 (1968) 1083-1096.

[27] A. Stanger, Nucleus-independent chemical shifts (NICS): distance dependence and revised criteria for aromaticity and antiaromaticity, The Journal of Organic Chemistry 71 (2006) 883-893.

[28] D. Pegu, J. Deb, C. Van Alsenoy, U. Sarkar, Theoretical investigation of electronic, vibrational, and nonlinear optical properties of 4-fluoro-4-hydroxybenzophenone, Spectroscopy Letters 50 (2017) 232-243.

[29] S. Suresh, A. Ramanand, D. Jayaraman, P. Mani, Review on theoretical aspect of nonlinear optics, Reviews on Advanced Materials Science 30 (2012) 175-183.

[30] K. Akhtari, K. Hassanzadeh, B. Fakhraei, H. Hassanzadeh, G. Akhtari,

S.A. Zarei, First hyperpolarizability orientation in [70] PCBM isomers: A DFT study, Computational and Theoretical Chemistry 1038 (2014) 1-5.

[31] R. Kakkar, Atomic and Molecular Spectroscopy: Basic Concepts and Applications, Cambridge University Press, 2015.

[32] V. Chahal, R. Kakkar, Theoretical investigation of the structural and electronic features of SLC-0111, a novel inhibitor of human carbonic anhydrase IX, and its anion, Structural Chemistry 32 (2021) 1843-1856.

[33] P.V.R. Schleyer, C. Maerker, A. Dransfeld, H. Jiao, N.J. van Eikema Hommes, Nucleus-independent chemical shifts: a simple and efficient aromaticity probe, Journal of the American Chemical Society 118 (1996) 6317-6318.

[34] C.P. Kelly, C.J. Cramer, D.G. Truhlar, Aqueous solvation free energies of ions and ion−water clusters based on an accurate value for the absolute aqueous solvation free energy of the proton, The Journal of Physical Chemistry B 110 (2006) 16066-16081.

[35] F.R. Dutra, C.D.S. Silva, R. Custodio, On the Accuracy of the Direct Method to Calculate p K a from Electronic Structure Calculations, The Journal of Physical Chemistry A 125 (2020) 65-73.

[36] R. Kakkar, M. Bhandari, R. Gaba, Tautomeric transformations and reactivity of alloxan, Computational and Theoretical Chemistry 986 (2012) 14-24.

[37] R.G. Parr, L. von Szentpály., S. Liu, Electrophilicity index, Journal of the American Chemical Society 121 (1999) 1922-1924.

[38] L. Domingo, P. Pérez, The nucleophilicity N index in organic chemistry, Organic and Biomolecular Chemistry 9 (2011) 7168-7175.

[39] H. Chermette, Chemical reactivity indexes in density functional theory, Journal of computational chemistry 20 (1999) 129-154.

[40] R.K. Roy, S. Krishnamurti, P. Geerlings, S. Pal, Local softness and hardness based reactivity descriptors for predicting intra-and intermolecular reactivity sequences: carbonyl compounds, The Journal of Physical Chemistry A 102 (1998) 3746-3755.

[41] T. Koopmans, About the assignment of wave functions and eigenvalues to the individual electrons of an atom, Physica 1 (1934) 104-113.

[42] M. Drissi, N. Benhalima, Y. Megrouss, R. Rachida, A. Chouaih, F. Hamzaoui, Theoretical and experimental electrostatic potential around the m-nitrophenol molecule, Molecules 20 (2015) 4042-4054.